

FIBER REINFORCED CONCRETE OF ENHANCED FIRE RESISTANCE FOR TUNNEL SEGMENTS

L. A. P. Lourenço, J. A. O. Barros¹, J. G. A. Alves

Synopsis: In the last decades, technical and scientific efforts have been done to increase the concrete strength, based on the assumption that more economic, lightweight, durable and good looking structures can be built. This strength enhancement, however, has been obtained by increasing the compactness of the concrete internal structure, resulting concretes with a void percentage much lower than the values observed in concretes of current strength classes. Research and fire accidents have shown that the concrete failure of structures exposed to fire is as explosive as high is the concrete strength class, since the concrete brittleness increases with the concrete compressive strength.

In the present work a fiber reinforced concrete of enhanced fire resistance was developed and its properties are characterized by experimental research. This concrete is intended to have enough resistance for the most structural engineering applications, while the performance of the fibrous reinforcement system was evaluated in terms of verifying its possibilities for replacing, partially or totally, conventional reinforcement used in concrete precast tunnel segments.

Keywords: High strength concrete, steel fibers, polypropylene fibers, high temperatures, residual mechanical properties, precast tunnel segments.

¹ Author to whom the correspondence should be sent (barros@civil.uminho.pt).

Lúcio Lourenço is a PhD Student in the Institute for Sustainability and Innovation in Structural Engineering (ISISE), Portugal. His main interests are the development of fiber reinforced concrete of enhanced fire resistance, material and structural characterization from experimental research, and numerical simulation by FEM analysis.

Joaquim Barros is an ISISE member, Associate Professor with Aggregation and Director of the Laboratory of the Structural Division of the Department of Civil Engineering, University of Minho. He is a member of ACI Committees 440 and 544, a member of TG 8.3 and *fib* TG 9.3, and a Council member of the IIFC. His research interests include structural strengthening, composite materials, fiber reinforced concrete and the development of constitutive models for the FEM analysis.

Adérito Alves is a Civil Engineer. His main interests are fire resistance of concrete structures and structural design of concrete structures.

DEVELOPMENT OF FIBER REINFORCED CONCRETE OF ENHANCED FIRE RESISTANCE

In the ambit of a research program involving Research Institutions and a Company dedicated to the construction of tunnel linings, a Fiber Reinforced Concrete of Enhanced Fire Resistance (FRCEFR) of enough resistance for precast tunnel segments was developed. This FRCEFR has a fibrous system that was designed to enhance the fire resistance of concretes of a characteristic compressive strength in the range of 60 to 80 MPa, and to increase significantly the concrete post-cracking residual strength, taking into account economic and technical requirements imposed by the Company, partner in this project. This fibrous system is composed by two types of fibers: a polypropylene fiber that, under the action of a fire, allows the formation of a system of micro-channels into the concrete microstructure, through which the water vapor can escape, reducing the possibility of concrete spalling; and a steel fiber that intends to increase both the post-cracking resistance of hardened concrete and the integrity of concrete when subjected to high temperatures. The steel fibers have also the purpose of replacing, partially or totally, the conventional steel reinforcement currently applied in precast tunnel segments.

For the selection of the nonmetallic type of fiber for the FRCEFR, an experimental program was carried out. Cubic specimens of 100 mm edge and beams of 250×50×60 mm³ were prepared to determine the influence of the maximum temperature exposure on the concrete compressive strength and on the flexural strength, respectively. A reference group of specimens without fibers (with the designation of Reference) and five groups of specimens were batched with the following distinct type of nonmetallic fibers: Ultrafiber cellulose fiber (length, l_f , of 2.1 mm); Asota AFC polypropylene (PP) fiber ($l_f = 6$ mm); Duro-Fibril PP fiber ($l_f = 12$ mm); Polyester ($l_f = 25$ mm); Cotton ($l_f = 25$ mm). In all these batches, a constant dosage of 2 kg per concrete m³ was used, since previous research (Lourenço *et al.*, 2005) showed that, above this content, the increment of costs does not justify the benefits in terms of fire resistance derived from fiber reinforcement. Furthermore, above this content, to assure appropriate fiber distribution, the mix

composition adjustments are significant for some types of fibers, which is an important concern when considerable changes in the production practices of the precast tunnel lining segments are not possible to implement. For comparison purposes, a concrete composition including Dramix® ZP 305 hooked ends steel fibers ($l_f = 30$ mm, diameter, d_f , of 0.55 mm, aspect ratio, l_f / d_f , of 55 and yield stress of 1100 MPa), as the unique fiber reinforcement system (dosage of 35 kg/m³), was also prepared. Details about the mix compositions can be found elsewhere (Lourenço *et al.*, 2005).

Fig. 1 shows that, if the mass loss of the Reference specimen is taken for basis of comparison, the steel fibers provided the lowest performance in this respect. In the nonmetallic fiber concrete the mass loss occurred at lower temperatures, due to the fact that micro channels formed into the concrete structure when nonmetallic fibers melted, resulting paths for the escape of the water vapor, with the consequent mass loss. The mass loss started at a temperature in the ambient chamber of about 150 °C. Explosive spalling occurred in Reference specimens, while fibrous specimens maintained their integrity up to a temperature of 750 °C. Therefore, all used nonmetallic fibers are able of improving the concrete fire resistance. However, only PP fibers allowed a relative easy fiber distribution into concrete. When compared to steel fiber reinforced concrete (SFRC) specimens, the higher mass loss registered in the nonmetallic fibrous specimens indicates that the used nonmetallic fibers are more effective in terms of assuring high volume of void micro-channels into the concrete microstructure for the escape of the water vapor.

The obtained results showed that, after high temperature exposure, concrete compressive strength ranged from 40% to 65% of the one of its homologous unheated specimen (Lourenço *et al.*, 2005). The influence of temperature was more pronounced in terms of the concrete flexural resistance, since a strength reduction higher than 80% was recorded. This experimental program revealed that PP fiber type is, amongst the used nonmetallic fibers, the one that provides higher benefits for the improvement of the concrete residual resistance when concretes are submitted to high temperatures. More details in this topic can be found elsewhere (Lourenço *et al.*, 2005).

INFLUENCE OF HIGH TEMPERATURES ON THE MECHANICAL PROPERTIES OF THE DEVELOPED FRCEFR

Compressive strength, elasticity modulus and flexural behavior

In the present Session, the experimental programs carried out to evaluate the residual compressive and flexural behavior of the developed FRCEFR are presented, and the main obtained results are analyzed. The tests were executed at 28 days after FRCEFR having been exposed to the following levels of temperature: 250°C, 500°C, 750°C and 1000°C. Cylinder specimens (150 mm diameter and 300 mm high) were used to determine both the concrete residual Young's modulus and the stress-strain relationship. Beam specimens (600×150×150 mm³) were also prepared to assess the residual concrete flexural behavior. One (PP1) and two (PP2) kg per concrete m³ of PP fibers (Duro-Fibril, $l_f = 6$ mm) were used to manufacture the tested specimens. The mix compositions are

included in Table 1. A content of 60 kg of Dramix® ZP 305 hooked ends steel fibers per concrete cubic meter was used in all compositions.

For each type of concrete and target test temperature, three cylinders and two beam specimens were tested, and the average of the corresponding results was used as the final values. Concrete specimens were heated, without any external applied load, at a constant rate of about 25 °C / min until the ambient temperature inside the furnace reaches the target test temperature. Then, the temperature was kept constant for 4 hours. The exposure to the 1000 °C level of temperature led to the destruction of the concrete specimens, therefore the residual behavior of these specimens was not possible to obtain. The variation of the Young's modulus, compressive and flexural strength with the variation of the target test temperatures are shown in Figs. 2 to 4. In these figures E_{cmT}^{res} and E_{cmT} are the Young's modulus at the T target test temperature and at the temperature of the laboratory natural environmental conditions (around 20 °C), respectively. Fig. 2 shows that the relative decrease of the concrete Young's modulus with the increase of the maximum temperature was almost similar for the three analyzed concrete compositions, but the concretes with cement type 42.5R showed a slight better performance in terms of retaining the relative residual Young's modulus. In terms of content of PP fibers, 2 kg/m³ provided higher retention of the relative residual Young's modulus up to of about 400 °C, than 1 kg/m³, but after this limit of maximum temperature the benefits of using a higher content of PP fibers seem to be marginal.

Figs. 3a to 3c show the damage induced by high temperatures on the compressive stress-strain response, which starts being intense above 250 °C. Up to this temperature, the initial Young's modulus seems to be not affected, and the compressive strength was only significantly reduced in the composition with 1 kg/m³ of PP fibers. Fig. 3d reveals that the decrease of relative concrete compressive strength due to the increase of concrete temperature exposure was not so pronounced in the developed FRCEFR, as it is predicted by the model proposed by EC2, mainly in FRCEFR reinforced with 2 kg/m³ of PP fibers.

The flexural tests were carried out according to the RILEM TC 162-TDF recommendations for the determination of the equivalent residual strength parameters, $f_{eq,2}$ and $f_{eq,3}$ that characterize the concrete flexural post-cracking behavior (Vandewalle *et al.*, 2000). From these tests the influence of the maximum temperature on peak load, F_p , was also evaluated. The obtained results, shown in Figs. 4 and 5, reveal that up to 250 °C the values of these parameters increased, but after this level of temperature they decreased significantly. This decrease was more pronounced in terms of peak load than in relation to the equivalent residual strength parameters. Fig. 4 also shows that the initial flexural stiffness was not affected up to 250 °C.

INVERSE ANALYSIS TO ASSESS THE INFLUENCE OF THE TEMPERATURE ON THE FRCEFR FRACTURE PARAMETERS

Based on the force-deflection curves obtained in the three point beam bending tests with FRCEFR specimens subjected to distinct levels of maximum temperature, an inverse analysis (Barros *et al.* 2007) was carried out to evaluate the influence of the maximum temperature on the values that define the crack stress-strain diagram that simulates the post-cracking behavior of the tested FRCEFR. The trilinear stress-strain diagram represented in Fig. 6 was used to simulate the crack opening and propagation, where G_f' is the mode I fracture energy and l_b is the crack band width that assures mesh objectivity under the framework of the nonlinear fracture mechanics, when using smeared crack models implemented into a FEM-based software (Bazant and Oh, 1983). The trilinear post-cracking diagrams that have best fitted the experimental force-deflection curves (Fig. 7) are represented in Fig. 8.

From Fig. 8a it is visible that, after crack initiation, a hardening phase occurred (first branch of the trilinear diagram), but for temperatures higher than 250 °C its amplitude decreased with the increase of the maximum temperature. The FRCEFR subjected to the maximum temperature of 750 °C presented an almost constant post-cracking residual strength. The influence of the maximum temperature on both the stress crack initiation ($\sigma_{n,1}^{cr}$) and fracture energy is represented in Fig. 8b, from which it can be verified that the fracture energy decreased with the increase of the maximum temperature, mainly between 250 °C and 500 °C. For the stress crack initiation, if the abnormal too low value obtained for 20 °C is not considered, a smooth decrease occurred up to 500 °C, followed by a significant decrease above this temperature. Therefore, up to 500 °C the brittleness of the FRCEFR increased significantly, since this concept has a direct quadratic proportionality with the tensile strength, f_{ct} , and an inverse linear proportionality with the fracture energy ($(l_{ch})^{-1} = f_{ct}^2 / (G_f E_c)$), where l_{ch} is the material characteristic length (Hillerborg *et al.* 1976)).

FIRE RESISTANCE OF TUNNEL SEGMENTS

Tunnel segments of distinct percentages of steel fibers and different steel reinforcement ratios were subjected to fire tests and, after having been cooled, their residual flexural resistance was assessed carrying out three point bending tests. The tunnel segments had dimensions of 1.20×2.45×0.35 m³, and thermocouples were installed at pre-selected points inside the specimen to measure the concrete temperature variation (Alves 2008).

Four tunnel segments were manufactured: a reference concrete specimen without fibers and with 110 kg/m³ of conventional steel bars (Specimen 1) arranged according to the disposition used in the construction of precast segments, by the Company associated to this research project; a second one (Specimen 2), with 75 kg/m³ of steel fibers and without steel bars; a third specimen with 45 kg/m³ of steel fibers and 51 kg/m³ of steel

bars (Specimen 3); and finally, a fourth specimen with 60 kg/m^3 of steel fibers and 35 kg/m^3 of steel bars (Specimen 4). In specimens 3 and 4 the steel bars form an embedded beam in the contour of the tunnel segments. High bond surface steel bars of a characteristic value of the yield stress of 500 MPa were used in the entire experimental program. The mix compositions of these tunnel segments are indicated in Table 2. DRAMIX® RC-80/60-BN hooked end steel fibres (SF) and polypropylene fibres Duro-Fibril (PF) were used in the FRC for these segments. Steel fibre has a length of 60 mm, a diameter of 0.75 mm, an aspect ratio of 80 and a yield stress of 1100 MPa. Polypropylene fibre has a length of 6 mm and a diameter of $31 \mu\text{m}$. A weight dosage of 2 kg/m^3 of polypropylene fibers was also added to the concrete of the specimens 2, 3 and 4. From compression tests with cylinders of 150 mm diameter and 300 mm height it was obtained (average of the results in two specimens for each fibrous composition) a compressive strength, at 28 days, of 62.8, 65.6 and 58.6 MPa for the FRCEFR reinforced with 45, 60 e 75 kg/m^3 of steel fibers, respectively.

Fire tests

The specimens, supported on a steel reaction frame, were tested in a fire resistance furnace capable of follow the ISO 834 curve. During the fire resistance tests, the elements were subjected to a constant load of 174 kN, according to a load configuration of four-line bending tests. This load level was determined in order to simulate, as closest as possible, the critical stress field that can exist in tunnel segments, at service load conditions. The axial stress, which always exists in this type of elements, was not simulated in the experimental tests due to the impossibility of materializing this load conditions with the available laboratory facilities. For the applied loading, a maximum flexural tensile stress of about 2.8 MPa was applied, which corresponds to the $f_{ctk,min}$ of a C50/60 concrete strength class, according to the CEB-FIP model code (1993).

After 10 minutes of fire exposure, a macro-crack occurred in Specimen 2, at the face turned to the fire, near its midspan. During the fire exposure, the width and the depth of this crack increased up to the flexural collapse of the specimen, which occurred after 110 minutes fire test initiation. During this period of fire exposure, the residual tensile strength of fibrous concrete decreased significantly (depending on the level of temperature installed on the materials), resulting a reduction on the flexural resistance of the tunnel segment cross section. Furthermore, since the applied load was maintained during the fire test, the specimen experienced an increase of deflection due to both effects of lost of flexural stiffness and creep, having specimen 2 failed prematurely.

The other elements resisted for more than 240 minutes without reaching the maximum deflection or speed of deformation indicated in EN 1363-1 for fire resistance tests (CEN, 1999).

Fig. 9 presents a synthesis of the results obtained in the fire resistance tests with FRCEFR tunnel segments subjected to the ISO 834 standard fire curve. Specimen 1 was the first to be tested and, due to deficient functioning of the supports, the test was interrupted at 200 minutes. A significant increase of the deflection rate is observed after 100 minutes of fire

exposure, which may be justified by an excessive deformation of the supports. This fact was solved for the subsequent tests. Specimen 3 and 4 presented the smallest deflection rates, which indicates that the reinforcement that combines steel fibers and bars placed in the contour of the specimen is appropriate in terms of retaining the stiffness of the structural element under fire conditions.

Fig. 9b evinces that fibers were effective in terms of offering resistance to temperature propagation. Due to the formation of a macro-crack in the Specimen 2, the thermocouples disposed near the failure crack registered an abrupt increment of temperature. From the analysis of the results obtained in these tests it was verified that, in general, the maximum temperature was registered in Specimen 1, followed by Specimens 3 and 4 with similar performance in this respect. Specimen 2 was excluded from this analysis, due to the fact that this test was interrupted at 110 minutes. A detailed analysis of the obtained results can be found elsewhere (Alves, 2008).

Residual flexural strength

The tunnel segments that did not collapse during fire test were, after cooled in the laboratory environment, tested under a three point load configuration, in order to evaluate their residual flexural resistance. The elements were tested under displacement control. The obtained force-deflection curves are represented in Fig. 10, from which it can be concluded that Specimen 1 presented the largest residual flexural resistance. The others specimens presented similar load carrying capacity. The Specimen 2 was not tested since, as already mentioned, it collapsed during the fire resistance test.

Residual indirect tensile strength

For each tunnel segment tested, 3 cores of 148 mm diameter and 350 mm depth were extracted to assess the indirect tensile strength along the thickness of the tunnel segment. Each core was divided in four cylinders of 75 mm height. The results presented in Fig. 11 show that fiber reinforcement was very effective in terms of retaining the tensile strength of tunnel segments submitted to fire (in this Fig. the depth was measured from the face turn to the fire).

CONCLUSIONS

From the obtained results it can be concluded that all used nonmetallic fibers are able of improving the concrete fire resistance, since explosive spalling was avoided. However, only PP fibers allowed a satisfactory and easy distribution into concrete. Using 1 kg of PP fibers per m³ of concrete, explosive spalling was avoided. Increasing the PP fiber dosage from 1 to 2 kg/m³, the compressive and the flexural residual concrete behavior was not significantly improved. However, in terms of the residual compressive strength up to a maximum temperature exposure of 500 °C, 2 kg/m³ of PP fibers had an appreciable higher contribution than 1 kg/m³. The highest difference was registered for a maximum temperature of 250 °C. In terms of residual flexural behavior, the peak force and the

equivalent residual strength parameters increased up to a maximum temperature exposure of 250 °C, but a significant reduction of the values of these properties occurred for higher temperatures, mainly the peak force.

Performing an inverse analysis with the results obtained in the flexural tests, it was verified that the maximum temperature exposure had induced a higher degradation in terms of fracture energy than in relation to the stress crack initiation, which means that the material brittleness increased with the maximum temperature exposure.

A series of fire resistance tests with tunnel segments submitted to ISO 834 curve and to a flexural loading configuration that introduces a maximum tensile stress of about 3 MPa was executed. From the variation of the temperature in the thermocouples it was concluded that the specimens with hybrid reinforcement (steel bars and steel fibers) had the best behavior in terms of offering resistance of temperature propagation. The flexural tests with these specimens, after having been submitted to the fire resistance tests, also showed that hybrid reinforcement is also a competitive reinforcement solution, since it assured an ultimate load that was almost the double of the service load. Indirect tensile tests with core cylinder specimens, extracted from the tunnel segments after having been submitted to fire and flexural tests, also showed that fibrous reinforcement system is very effective in terms of retaining the concrete tensile strength.

ACKNOWLEDGEMENTS

The authors wish to acknowledge the support provided by the Portuguese Science and Technology Foundation (FCT) by means of the project POCTI/ECM/57518/2004 “FICOFIRE - High performance fiber reinforced concrete of enhanced fire resistance”, as well as the support of Spie Batignolles Company.

REFERENCES

Alves, A.J.G., “Fire behavior of fiber reinforced concrete”, MSc Thesis, University of Coimbra, in preparation (in Portuguese)

Barros, J.A.O.; Pereira, E.N.B.; Gouveia, A.V.; Azevedo, A.F.M., “Numerical simulation of thin steel fiber self-compacting concrete structures”, ACI 435/544 Fall 2007 Puerto Rico Session 1: Deflection and stiffness issues in FRC and thin structural elements (Structural Implications and Material Properties), in CD, 25 pages, October 2007.

Bazant, Z.P. and Oh, B.H., “Crack band theory for fracture of concrete”, *Materials and Structures*, RILEM, 16(93), 155-177, 1983.

CEB-FIP Model Code 1990, “Design Code.” *Comite Euro-International du Béton, Bulletin d’Information n° 213/214*, 437 pp, 1993.

CEN, EN 1363-1, “Fire Resistance Tests – part 1: General Requirements”, August 1999

Eurocode 2, “Design of concrete structures - Part 1-2: General rules - Structural fire design”, European Committee for Standardization, 2003.

Eurocode 4, “Design of composite steel and concrete structures - Part 1-2 : General rules - Structural fire design”, prEN1994-1-2, English version, 2003.

Hillerborg, A.; Mod er, M.; Petersson, P.E., “Analysis of crack formation and crack growth in concrete by means of fracture mechanics and finite elements”, Cement and Concrete Research, Vol. 6, pp. 773-782, 1976.

International Organization for Standardization, “Fire-Resistance Tests – Elements of Building Construction. Part 1. Part 1: General Requirements”, ISO 834-1. ISO. Geneva, 1999.

Lourenço, L.A.P., Barros, J.A.O., & Souto, P., “Concrete composition of enhanced fire resistance concrete for tunnel segments – part I”, Technical report 05-DEC/E-32, Dep. of Civil Eng., University of Minho, December 2005, 42 pages. (in Portuguese).

Lourenco, L.A.P.; Barros, J.A.O.; Santos, S.P.F., "High Strength and Ductile Fibrous Concrete of Enhanced Fire Resistance", Int. Conf. Materiais 2007, FEUP, 5p, 2007.

Vandewalle, L. et al., “Test and design methods for steel fiber reinforced concrete. Recommendations for σ - ε design method”, Materials and Structures, 33(226), 75-81, Mar-Apr. 2000.

TABLES AND FIGURES

List of Tables:

Table 1: FRCEFR compositions (per concrete cubic meter)

Table 2 – Concrete compositions of the tunnel segments (per m³)

Table 1: FRCEFR compositions (per concrete cubic meter)

Cement ⁽¹⁾	Limestone Filler	Water	Super plasticizer	Fine Sand	Coarse Sand	Crushed Calcareous 5-12 mm	Crushed Calcareous 14-20 mm	Steel Fibers
(C)	(LF)	(W)	(SP)	(FS)	(CS)	(CA_1)	(CA_2)	(SF)
[kg]	[kg]	[dm ³]	[dm ³]	[kg]	[kg]	[kg]	[kg]	[kg]
300.2	228.0	120.5	7.0	533.6	457.6	295.0	294.3	60.0

(1) Type I 42.5R and type I 52.5R; SP- Sika ViscoCrete® 3002 HE

Table 2 – Concrete compositions of the tunnel segments (per m³)

	C	W	SP⁽¹⁾	LF	FS	CS	CA_1	CA_2	SF	PF
	(kg)	(kg)	(dm³)	(kg)	(kg)	(kg)	(kg)	(kg)	(kg)	(kg)
Specimen 1	205	165	5.13	-	580.0	220.0	530.0	540.0	-	-
Specimen 2					550.5	451.8	289.7	289.4	75	
Specimen 3	360	114	8.03	247	524.5	460.3	297.3	297.1	45	2
Specimen 4					533.6	457.6	294.5	294.3	60	

⁽¹⁾ Sika ViscoCrete® 3002 HE

List of Figures:

Fig. 1: Mass loss (heating phase)

Fig. 2: Influence of the level of temperature exposure on the residual Young's modulus

Fig. 3: Influence of the level of temperature exposure on the residual compressive behavior

Fig. 4: Influence of the level of temperature exposure on the residual flexural behavior

Fig. 5: Influence of the level of temperature exposure on the residual equivalent flexural tensile strength parameters

Fig. 6: Trilinear stress-strain diagram for modeling the fracture mode I.

Fig. 7: Inverse analysis

Fig. 8: Influence of the maximum temperature on the: a) constitutive law that simulates the crack initiation and crack propagation; b) crack stress initiation and fracture energy

Figure 9: Fire resistance tests: a) Variation of midspan displacement during test; b) Concrete temperature variation at the center and the depth of 32 cm of the tunnel segment

Fig. 10: Experimental load versus mid span displacement for the tunnel segments after having been exposed to ISO 834 curve

Fig. 11: Indirect tensile strength tests

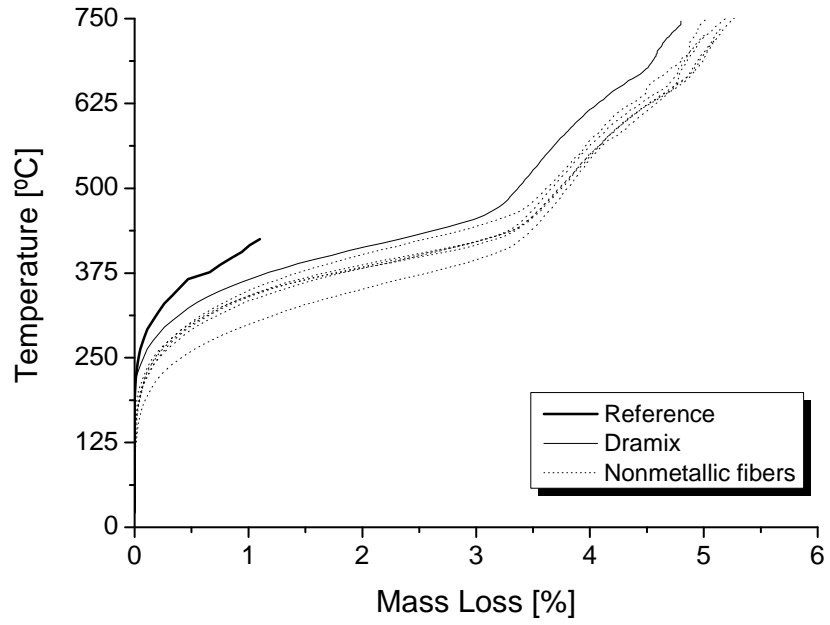


Fig. 1: Mass loss (heating phase)

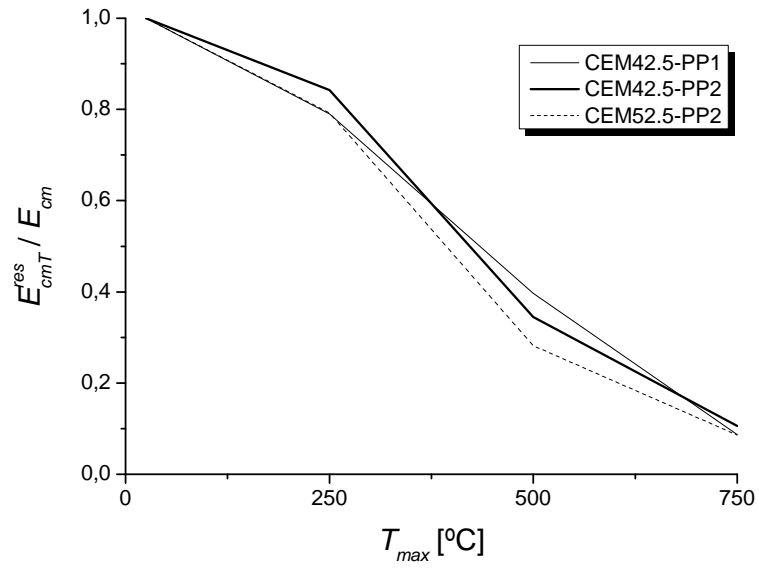


Fig. 2: Influence of the level of temperature exposure on the residual Young's modulus

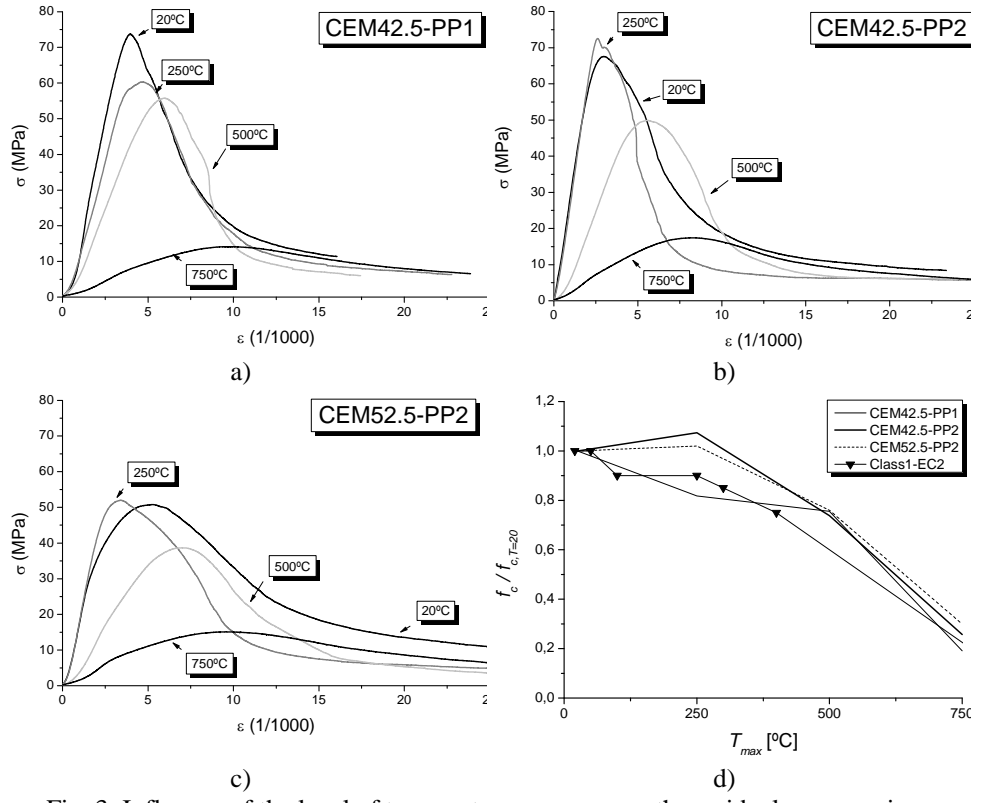


Fig. 3: Influence of the level of temperature exposure on the residual compressive behavior

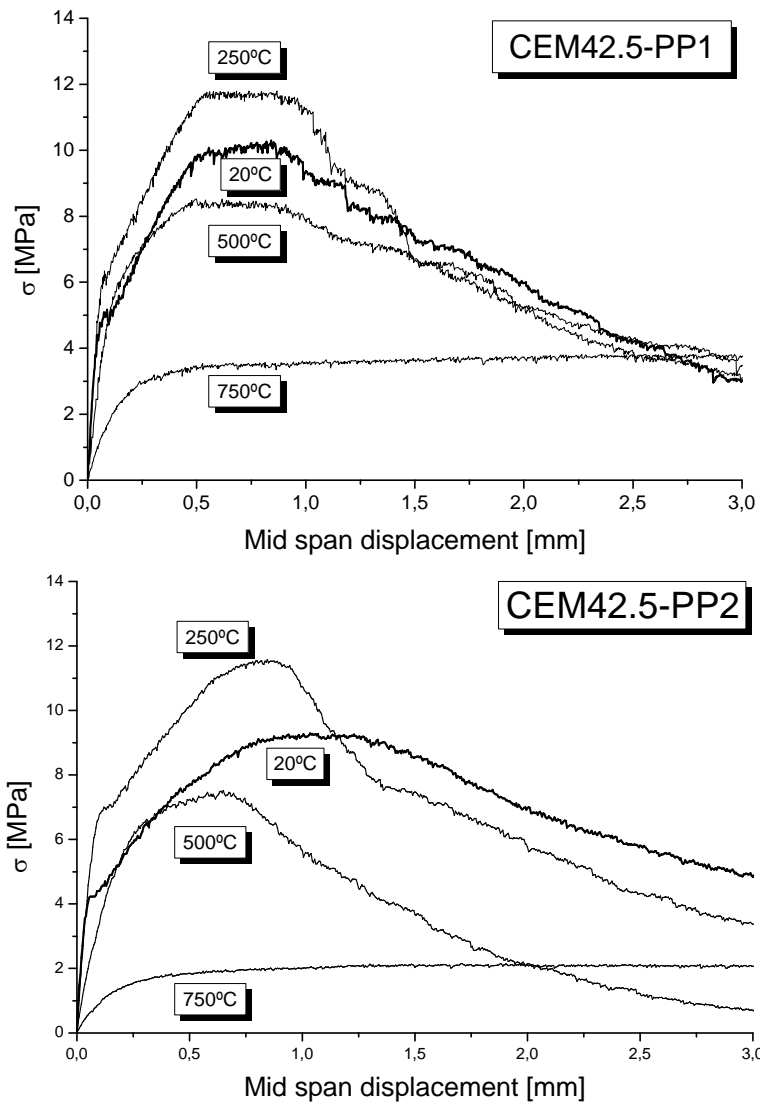


Fig. 4: Influence of the level of temperature exposure on the residual flexural behavior

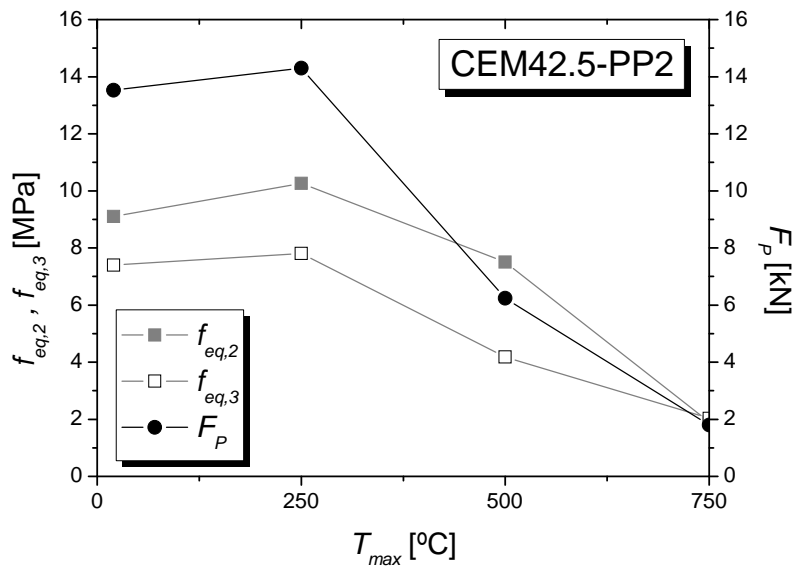
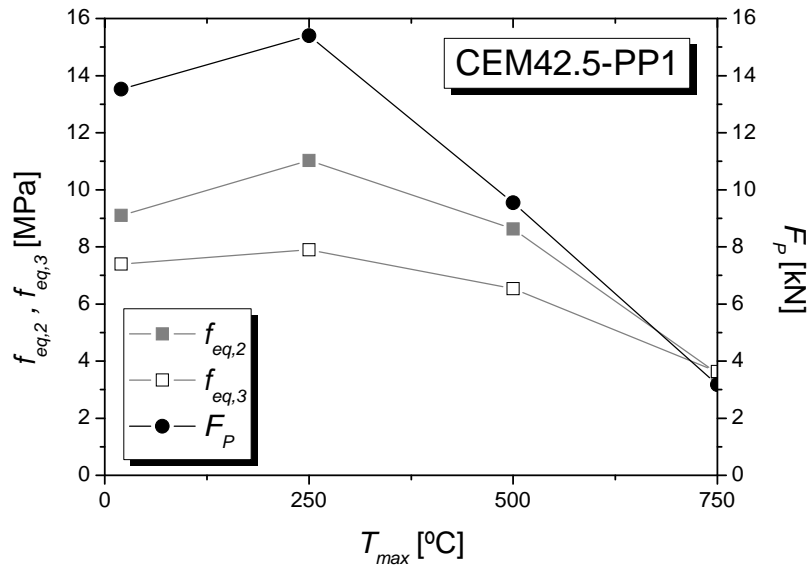


Fig. 5: Influence of the level of temperature exposure on the residual equivalent flexural tensile strength parameters

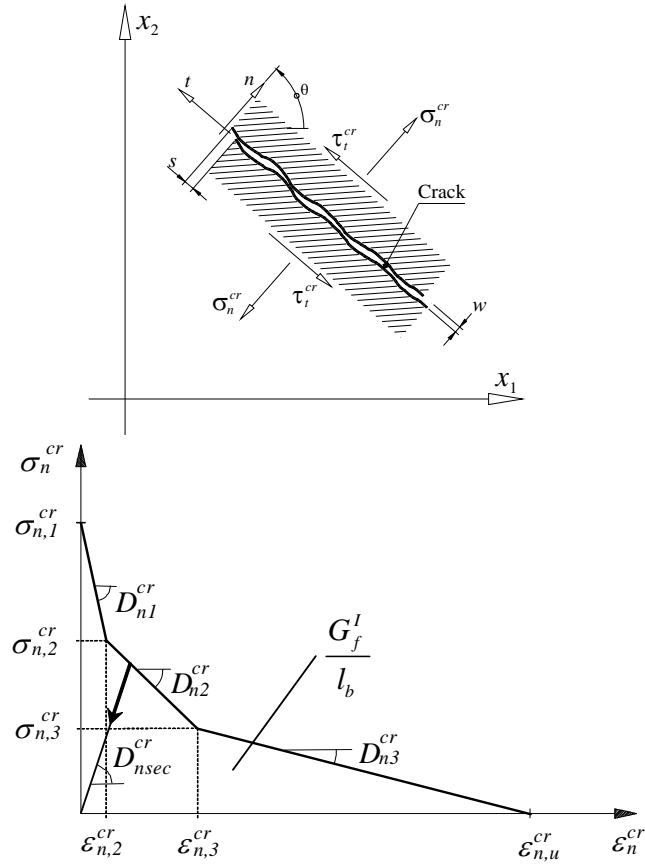


Fig. 6: Trilinear stress-strain diagram for modeling the fracture mode I

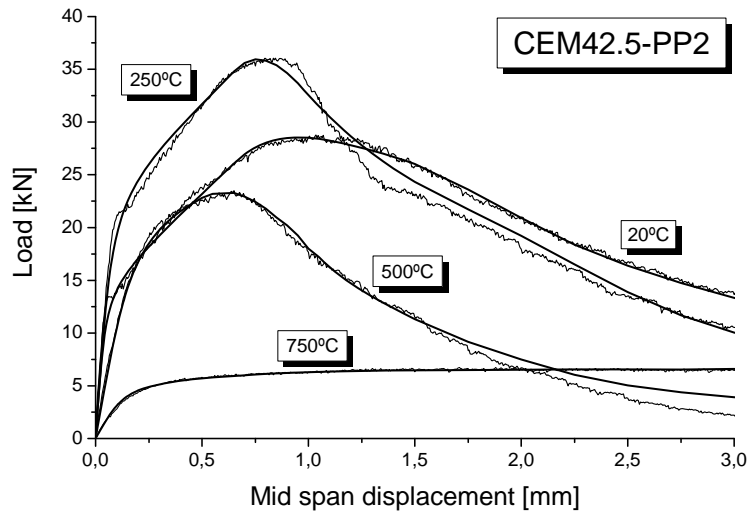
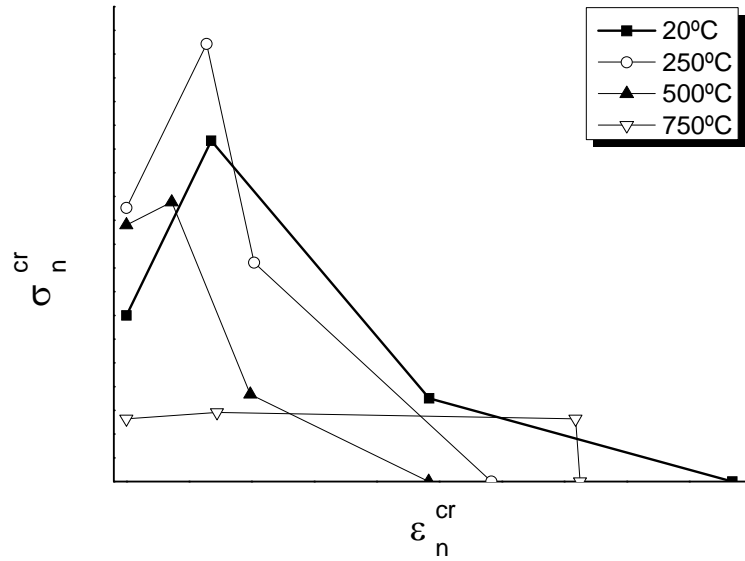
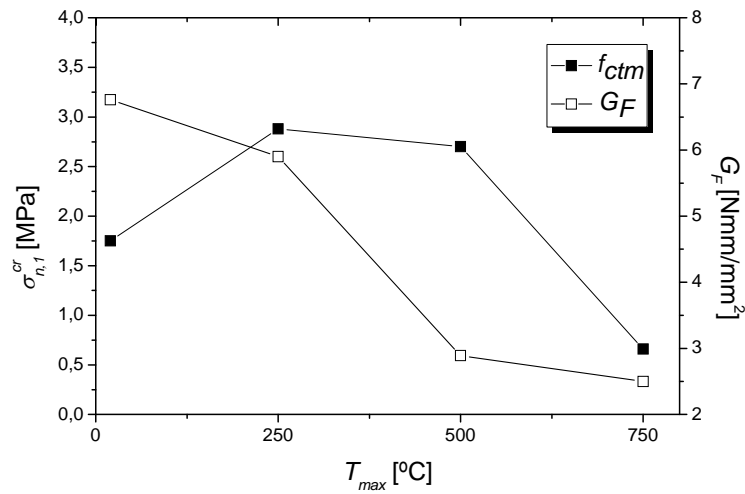


Fig. 7: Inverse analysis

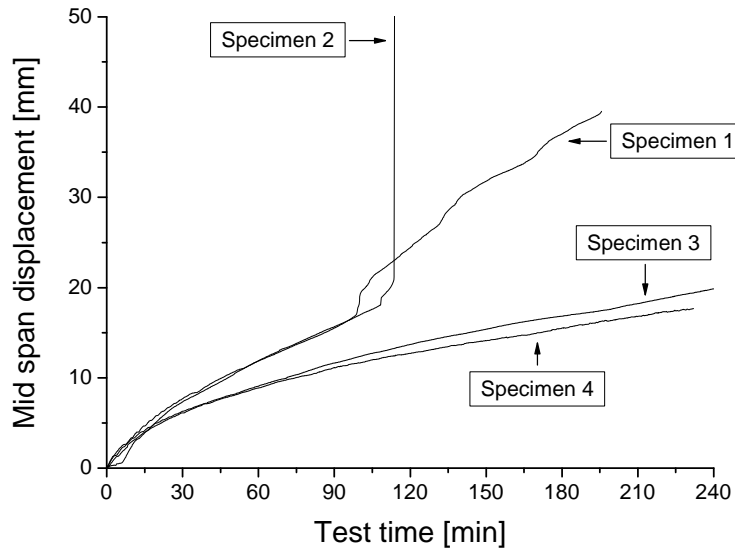


a)

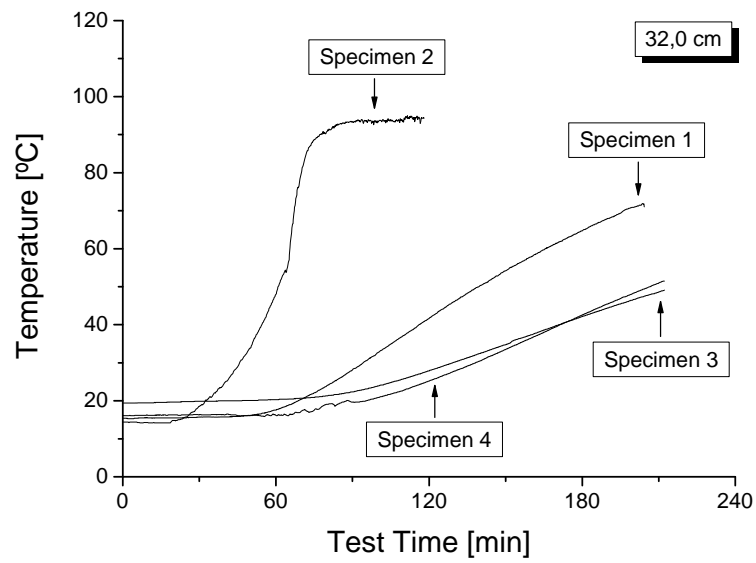


b)

Fig. 8: Influence of the maximum temperature on the: a) constitutive law that simulates the crack initiation and crack propagation; b) crack stress initiation and fracture energy



a)



b)

Figure 9: Fire resistance tests: a) Variation of midspan displacement during test; b) Concrete temperature variation at the center and the depth of 32 cm of the tunnel segment

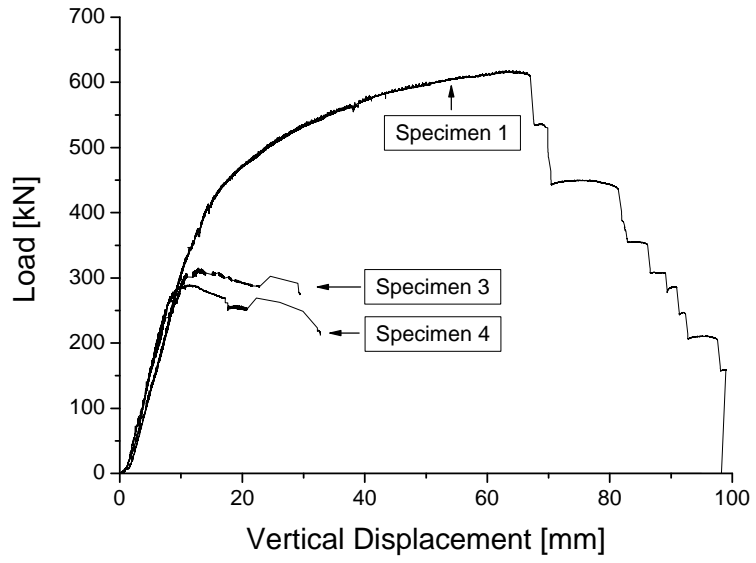


Fig. 10: Experimental load versus mid span displacement for the tunnel segments after having been exposed to ISO 834 curve

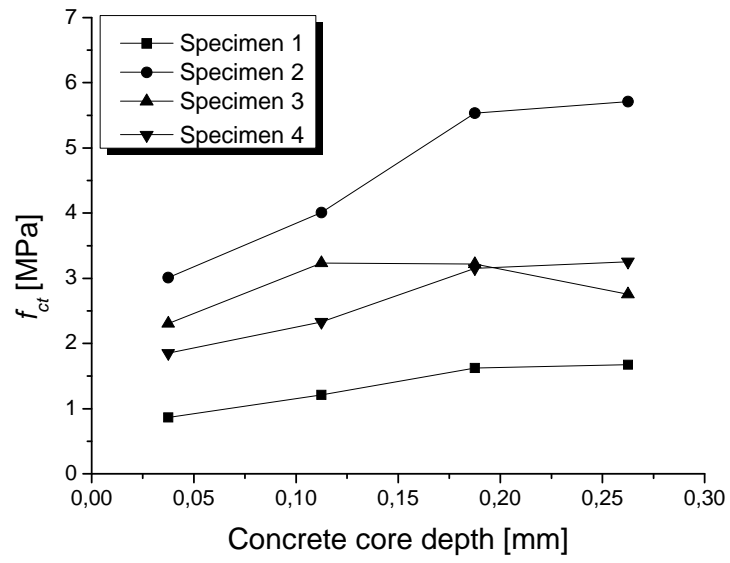
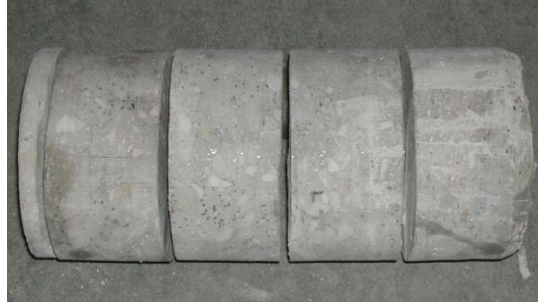


Fig. 11: Indirect tensile strength tests